Biochemical and Biophysical Research Communications 400 (2010) 157–163

Contents lists available at ScienceDirect

Biochemical and Biophysical Research Communications

journal homepage: www.elsevier.com/locate/ybbrc

Isolation and characterization of a novel peptide, osteoblast activating peptide (OBAP), associated with osteoblast differentiation and bone formation

Nobuhiro Fukushima [a,*], Koji Hiraoka [a], Isao Shirachi [a], Masayasu Kojima [b], Kensei Nagata [a]

[a] Department of Orthopaedic Surgery, Kurume University School of Medicine, Kurume, Fukuoka 830-0011, Japan
[b] Molecular Genetics, Institute of Life Science, Kurume University, Kurume, Fukuoka 839-0861, Japan

ARTICLE INFO

Article history:
Received 5 August 2010
Available online 13 August 2010

Keywords:
Peptide
Osteoblast
Differentiation
Bone mineral density (BMD)

ABSTRACT

A long-standing goal in bone loss treatment has been to develop bone-rebuilding anabolic agents that can potentially be used to treat bone-related disorders. To purify and isolate a novel anabolic that acts to osteoblasts, we monitored changes in intracellular calcium concentrations ($[Ca^{2+}]i$). We identified a novel, 24 amino-acid peptide from the rat stomach and termed this peptide osteoblast activating peptide (OBAP). Furthermore, we examined the effects of OBAP in osteoblasts. First, osteoblast differentiation markers (alkaline phosphatase [ALP], osteocalcin [OCN]) were analyzed using quantitative RT-PCR. We also examined the ALP activity in osteoblasts induced by OBAP. OBAP significantly increased the expression of osteoblast differentiation markers and the activity of ALP *in vitro*. Next, to address the *in vivo* effects of OBAP on bone metabolism, we examined the bone mineral density (BMD) of gastrectomized (Gx) rats and found that OBAP significantly increased BMD *in vivo*. Finally, to confirm the *in vivo* effects of OBAP on bone, we measured serum ALP and OCN in Gx rats and found that OBAP significantly increased serum ALP and OCN. Taken together, these results indicate that the novel peptide, OBAP, positively regulates bone formation by augmenting osteoblast differentiation. Furthermore, these results may provide a new therapeutic approach to anabolically treat bone-related disorders.

1. Introduction

Osteoporosis is characterized by low bone mass and structural bone deterioration, both of which are associated with reduced bone strength and an increased risk of fracture. In the United States alone, 10 million people are estimated to have osteoporosis, and osteoporosis contributes to 1.5 million fractures each year [1]. Bone undergoes a normal remodeling process, mediated by the coordinated actions of osteoclasts and osteoblasts. Bone loss and skeletal fragility in osteoporosis are caused by an imbalance in bone remodeling, in which the rate of osteoclast-mediated bone resorption is higher than the rate of osteoblast-mediated bone formation. A variety of therapeutics are currently used to treat osteoporosis, with the vast majority being antiresorptive agents that exert their clinical effects by decreasing the rate of bone resorption, thereby preventing further bone loss and reducing fractures [2]. Along with ongoing efforts to develop improved antiresorptive agents, a long-standing goal has been to develop therapeutics that can stimulate bone formation to increase bone mass and bone strength. It is thought that such bone-rebuilding anabolics could provide important treatment options, not only for low bone mass conditions but also for fracture healing, orthopaedic procedures, etc. Currently, the only approved bone anabolic agents for osteoporosis are full-length and truncated PTH, both of which are administered by daily subcutaneous injections [2]. Therefore, it is important to identify new bone anabolic agents.

Here, we report the purification and isolation of a novel peptide that acts to osteoblasts. In addition, we demonstrate that this novel peptide regulates osteoblast activation and bone formation.

2. Materials and methods

2.1. Animals

Sprague–Dawley (SD) rats (Charles River Co., Yokohama, Japan) were used to purify the peptide and to conduct both osteoblast-like cell culture experiments and *in vivo* studies. The rats were housed in a regulated environment (22 ± 2 °C, 55 ± 10% humidity, 12-h light, 12-h dark cycle with lights on at 0700 h) with free access to food and water. All experiments were conducted in accordance with the Japanese Physiological Society's guidelines for animal care.

2.2. Cell culture

Primary osteoblast-like cells were isolated by digesting a 21-day-old fetal rat calvaria with collagenase (Sigma Chemical

* Corresponding author. Address: Department of Orthopaedic Surgery, Kurume University School of Medicine, 67 Asahi-machi, Kurume, Fukuoka 830-0011, Japan. Fax: +81 942 350709.
E-mail address: fukushima_nobuhiro@kurume-u.ac.jp (N. Fukushima).

0006-291X/$ - see front matter © 2010 Elsevier Inc. All rights reserved.
doi:10.1016/j.bbrc.2010.08.036

Co., St. Louis, MO, USA) as previously described [3,4]. Digests 3–5 were pooled and grown in 10-cm cell culture plates in primary culture media consisting of α-Minimal Essential Medium (α-MEM; containing L-glutamine and nucleosides) (Life Technologies-GIBCO, Cergy Pontoise, France) supplemented with 10% fetal bovine serum (Thermo Trace, Melbourne, Australia) and antibiotics, including 100 μg/ml penicillin G (Life Technologies-GIBCO), 50 μg/ml streptomycin sulfate, and 0.3 μg/ml Fungizone (Life Technologies-GIBCO). Cells were grown to confluence before experimentation.

UMR-106 cells, a rat osteoblastic cell line, were obtained from Dainippon Pharmaceutical Co. (Osaka, Japan). Cells were plated in 10-cm plates at a density of 2×10^5 cells/plate and maintained in Dulbecco's Modified Eagle's Medium (DMEM) (Life Technologies-GIBCO) supplemented with 10% fetal bovine serum and antibiotics.

All cultures were incubated at 37 °C in a humidified atmosphere of 95% air and 5% CO_2.

2.3. Purification of the novel peptide

The novel peptide was isolated and purified by the same method as previously described [5]. A fresh rat stomach (50 g) was diced and boiled for 5 min in five volumes of water to inactivate the intrinsic proteases. The solution was adjusted to 1 M AcOH, 20 mM HCl. Peptides were extracted by homogenizing with a Polytron mixer. The extracts were centrifuged for 30 min at 11,000 rpm, and the supernatants were concentrated to approximately 40 ml with an evaporator. The residual concentrate was precipitated with 66% acetone. After the precipitates were removed, the acetone-containing supernatant was evaporated. The solution was loaded onto a 10-g cartridge of Sep-Pak C18 (Waters), which was pre-equilibrated with 0.1% trifluoroacetic acid (TFA). The Sep-Pak cartridge was washed with 10% CH_3CN/0.1% TFA, and then eluted with 60% CH_3CN/0.1% TFA. The eluate was evaporated and lyophilized. The residual materials were redissolved in 1 M AcOH and then adsorbed on a SP-Sephadex C-25 column (II + form) that was pre-equilibrated with 1 M AcOH. Successive elution with 1 M AcOH, 2 M pyridine and 2 M pyridine AcOH (pH 5.0) yielded three fractions of SP-I, SP-II, and SP-III. The lyophilized SP-III fraction was applied on a Sephadex G-50 gel-filtration column. A portion of each fraction was subjected to the intracellular calcium concentration ($[Ca^{2+}]i$)-change assay using UMR-106 cells. Active fractions (43–48) were then separated by reverse-phase high-performance liquid chromatography (HPLC) using a symmetry300 C18 column (3.9 × 150 mm; Waters). The active fractions were further fractionated manually.

2.4. Structural analysis

The amino-acid sequence of the peptide was analysed with a protein sequencer (494; Applied Biosystems, Foster City, USA). The molecular weight was determined using MS. The fully protected peptide was synthesized by the Fmoc solid-phase method on a peptide synthesizer (433A; Applied Biosystems). Purified peptides were compared to synthetic peptides by reverse-phase HPLC. The activities of the novel peptide, HPLC-fractionated peptides, and the synthetic peptides were examined by monitoring the effects of these samples in the $[Ca^{2+}]i$-change assay.

2.5. Changes in intracellular Ca^{2+} concentrations

Changes in $[Ca^{2+}]i$ were measured using the FLEXstation Calcium Assay Kit (Molecular Devices), fluorescent dye Fluo-4 AM (Molecular Probes), and black-walled, clear-bottomed 96-well microplates (Costar, cat# 3603 and Greiner, E&K cat# 655090). Compound plates used were 96-well, V-bottomed, clear polypropylene plates (E&K, cat# 651201). A 1X Reagent Buffer containing 1× Hank's Balanced Salt Solution and 20 mM HEPES pH 7.4 was used to wash cells, dilute compound, and dissolve dye solutions. All buffers contained a final concentration of 2.5 mM probenecid in order to inhibit endogenous efflux pumps. Cells were seeded the night before the experiment at 5×10^4 cells/well in a volume of 100 μl per well of a 96-well microplate. Cells were incubated at 37 °C in 5% CO_2 overnight. The next day, the cells were incubated with Fluo-4 dye loading buffer at room temperature for 1 h. Then, the Fluo-4 dye-loaded cells were manually washed three times with 1× Reagent Buffer, and 100 μl of 1× Reagent Buffer was added to the wells. The compound was added to the plates of cells via FLEXstation and subsequent changes in fluorescent signals were monitored.

2.6. Cell proliferation assays

Primary osteoblast-like cells were seeded in 96-well plates at a density of 6000 cells/well. After 24 h, the media was changed to serum-free medium with 1% bovine serum albumin, and the cells were incubated for an additional 24 h before the experimental compounds were added.

The relative number of viable cells in each well was determined after a 48-h incubation with the compounds using the cell count reagent SF (Nacalai Tesque, Kyoto, Japan), 2-(2-methoxy-4-nitrophenyl)-3-(4-nitrophenyl)-5-(2,4-disulfophenyl)-2H-tetrazolium, monosodium salt (WST-8). Briefly, 10 μl of the WST-8 solution was added to each well, including three wells containing medium alone that were used to subtract the background fluorescence. Then, the cells were incubated at 37 °C for 1 h. The absorbance at 450 nm in each well was determined using a microplate reader, model 550 (Bio-Rad Laboratories, Hercules, CA, USA). This technique produces a linear relationship between the number of viable cells and the absorbance at 450 nm.

2.7. Assessment of the expression of osteoblast differentiation markers

Cells in 6-well plates were treated with or without peptide (10^{-4} or 10^{-5} M) and then analyzed after 3 and 14 days of *in vitro* culture. Cells were plated at a density of 4×10^4 cells/well and grown until they reached confluency, which was designated day 0. Cells were grown in primary culture media with 50 μg/ml ascorbic acid (Sigma Chemical Co.) and 10 mmol/L β-glycerophosphate (Sigma Chemical Co.). Total RNA was extracted from the cell pellets using an RNeasy Mini kit (Qiagen, Valencia, CA, USA) according to the manufacturer's instructions. cDNA was synthesized from 2 μg of total RNA using the Super Script Preamplification System for First-Strand cDNA Synthesis Kit (Life Technologies-GIBCO, Cergy Pontoise, France). cDNA was analyzed by quantitative real-time PCR using the ABI PRISM 7700 sequence detection system (Applied Biosystems). Specific primers that produce short PCR products suitable for SYBR-Green detection were designed using Primer Express software (version 1.0, PE Applied Biosystems). The primer sequences were as follows: Runx2 (Runx2; 67-bp product; GenBank accession no. AF053953), 5′-GCTTCATTCGCCTCACAAACA-3′ (sense) and 5′-TGCTGTCCTCCTGGAGAAAGTT-3′ (antisense); alkaline phosphatase (ALP; 101-bp product; GenBank accession no. J03572), 5′-CGTCTCCATGGTGGATTATGC-3′ (sense) and 5′-TGGCAAAGACCGCCACAT (antisense); osteocalcin (OCN; 63-bp product; GenBank accession no. X04141), 5′-GAGCTAGCGGACCACATTGG-3′ (sense) and 5′-CCTAAACGGTGGTGCCATAGA-3′ (antisense); and beta-actin (β-actin; 67-bp product; GenBank accession no. NM031144), 5′-TTCAACACCCCAGCCATGT-3′ (sense) and 5′-GTGGTACGACCAGAGGCATACA-3′ (antisense). Samples were examined in triplicate. The reaction volume was 50 μl and included 3 μl diluted cDNA (1:30), 10 μl SYBR green buffer, and 10 pmol of each primer. The samples were subjected to 45 cycles of amplification at 95 °C for 15 s, followed

by 52 °C for 60 s. The concentration of amplified cDNA in each sample was calculated relative to that of β-actin cDNA. After RT-PCR amplification, a dissociation analysis was performed to ensure that only one product was amplified in each PCR reaction. Products were also separated on a 2% agarose gel to confirm that reaction produced a single, correctly sized product.

2.8. Alkaline phosphatase (ALP) activity

The dose-dependent effects of the novel peptide were analyzed after a 5-day incubation with or without the peptide (10^{-4} or 10^{-5} M). ALP activity was analyzed histochemically using an alkaline phosphatase kit (WAKO Pure Chemical Industry, Osaka, Japan). Briefly, assay mixtures containing 0.1 M 2-amino-2-methyl-1-propanol, 1 mM $MgCl_2$, 8 mM p-nitrophenyl phosphate disodium, and cell homogenates were incubated for 5 min at 37 °C, after which the reaction was stopped with 0.1 N NaOH and the absorbance at 405 nm was measured. A standard curve was prepared with p-nitrophenol. Each value was normalized to the total protein concentration in the cell layer, which was measured by the Lowry method using a protein assay kit (Bio-Rad Laboratories, Hercules, CA, USA) and BSA as a standard.

2.9. Bone densitometry and μCT

We used gastrectomized (Gx) rats as an osteoporosis model. Gastrectomies were performed by a total resection of the stomach of 5-week-old male SD rats. Two weeks after recovering from the surgery, the gastrectomized (Gx) rats were randomly divided into two groups: Gx with vehicle and Gx with peptide.

Gx rats were infused intraperitoneally with the peptide ($n = 4$) (0.2 mg/kg per hour) or saline ($n = 5$) using osmotic minipumps (Alzet; Alza Corp., Palo Alto, CA, USA). We measured the body weight and food intake of the rats daily. After 4 weeks of treatment, the BMD of the femur was measured by dual-energy X-ray absorptiometry (DXA; model DCS-600; Aloka, Tokyo, Japan). In addition, we obtained two-dimensional images of the distal femurs by microcomputed tomography (μCT, Scan Xmate-L090, Comscan).

2.10. Assay for serum chemistry

Just before death, blood samples were taken, and serum was prepared. The osteocalcin (OC) levels in the serum were determined by ELISA with a rat OCN immunoassay kit (R&D Systems). Serum ALP was measured with an alkaline phosphatase kit. Assays were performed according to the manufacturer's recommendations.

2.11. Statistical analysis

Data are presented as the mean ± SD. A two-factor analysis of variance (ANOVA) was used to determine if differences between mean values were statistically significant, and $P < 0.05$ was considered statistically significant.

3. Results

3.1. Isolation of a novel peptide

Osteoblasts were monitored for changes in $[Ca^{2+}]i$ that were induced by tissue extracts from a rat stomach. Because the highest activity was detected in stomach extracts, these extracts were further purified by successive chromatography, including Sephadex G-50 gel filtration and reverse-phase HPLC (Fig. 1A and B). Gel filtration showed that fractions with a relative molecular mass of ~3000 potently increased $[Ca^{2+}]i$. Active fractions (fractions 43–48) were further purified by RP-HPLC to yield 20 μg of pure peptide from 50 g of rat stomach tissue (Fig. 1C).

3.2. Structural analysis of the novel peptide

Protein sequence analysis revealed that the amino-acid sequence of the purified peptide was LDLNLDLSKFRLPQPSSGRESPRH (Fig. 1D). The calculated mass of the novel peptide was 2763.4. To confirm that the native and synthetic peptides had similar structures, the peptides were analyzed by HPLC. The elution profiles of both the native and synthetic peptide were identical by C-18 reverse-phase. Moreover, mixtures of the native and synthetic

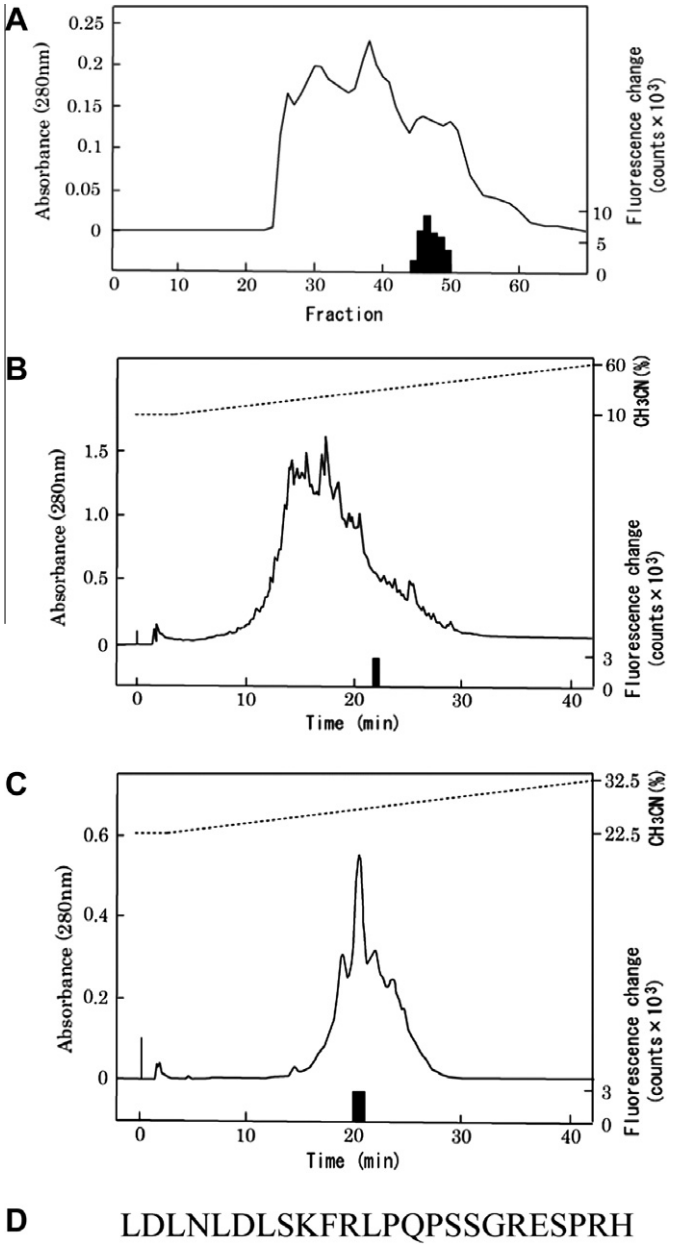

Fig. 1. Purification of the novel peptide. (A) Sephadex G-50 gel filtration of the SP-III fraction from 50 g of rat stomach. The black bars indicate the changes in fluorescence due to the increase in $[Ca^{2+}]i$ in UMR-106 cells. The active fractions eluted at approximately M_r 3000. (B) Reverse-phase HPLC of the active fractions in A. The broken line indicates the concentration of CAN in the eluting solvent. Bioactive fractions are represented by black bars. (C) Final purification by reverse-phase HPLC of the active fractions in B. (D) Structure of the novel peptide.

peptides eluted as a single peak (Fig. 2A). Next, to confirm that the native and synthetic peptides have similar effects, the peptides were analyzed in the $[Ca^{2+}]$i-change assay. The native and synthetic peptides produced similar $[Ca^{2+}]$i changes (Fig. 2B). These results confirmed the sequence of the peptide. As this peptide acts on osteoblasts, we termed this peptide osteoblast activating peptide (OBAP).

3.3. Effects of the novel peptide on $[Ca^{2+}]$i in cells

A novel peptide potently induced an increase in $[Ca^{2+}]$i in UMR-102 cells, whereas other peptides such as neuromedin that acts through GPCRs had no effect on cells under the same conditions (data not shown). OBAP induced $[Ca^{2+}]$i in primary osteoblasts and osteoblast-like cells but not RAW264.5 or CHO cells (Fig. 3A). This peptide also induced a dose-dependent increase in $[Ca^{2+}]$i (Fig. 3B).

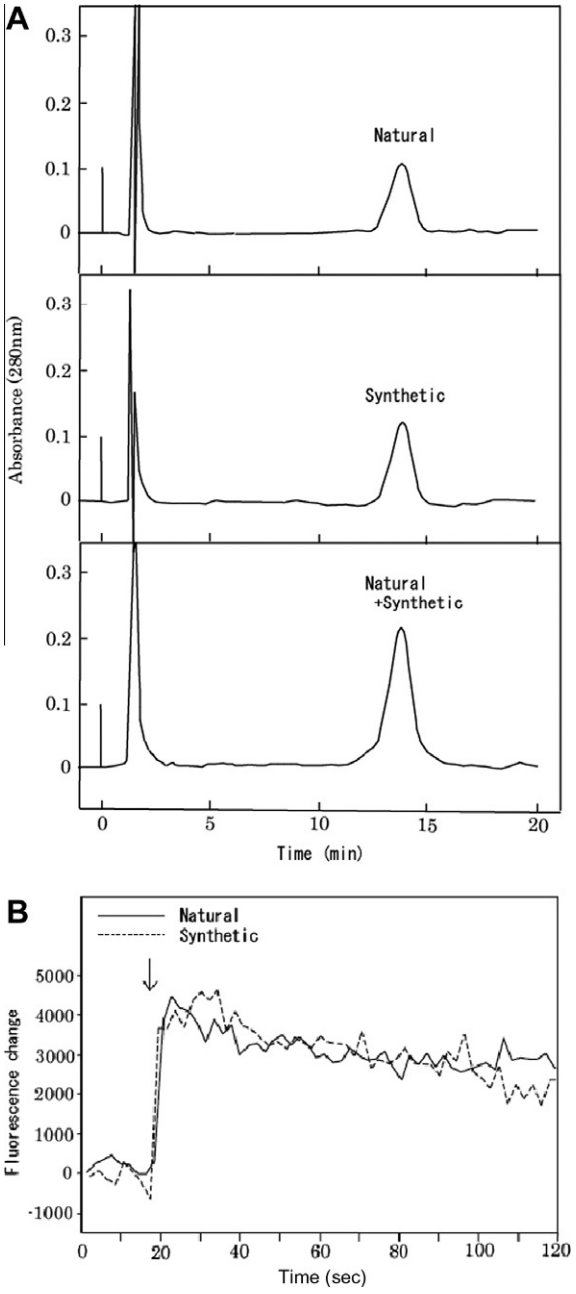

Fig. 2. Comparison of the natural and synthetic peptides. (A) Comparison of the elution profiles of natural, synthetic, and mixed peptides applied to reverse-phase HPLC. (B) Time courses of $[Ca^{2+}]$i changes in UMR-106 cells that were treated with the natural and synthetic peptides. Each peptide (2×10^{-4} M) was added at the time indicated by the arrow.

3.4. Effects of the novel peptide on osteoblast proliferation

Next, to assess the effects of the novel peptide on primary osteoblast-like cells, we measured cell viability in response to peptide treatment. In these assays, OBAP did not affect cell proliferation (data not shown).

3.5. Effects of the novel peptide on osteoblast differentiation

To further examine the effects of OBAP on osteoblast differentiation, we analyzed the expression of several markers of osteoblast differentiation, including Runx2, ALP and OCN, by quantitative RT-PCR. The expression of Runx2, a transcriptional factor necessary for osteoblast differentiation, was not significantly changed (data not shown). However, compared to vehicle-treated cells, 10^{-5} and 10^{-4} M OBAP significantly increased the expression of the early osteoblast differentiation marker, ALP, by up to 2.26- and 3.07-fold, respectively, at day 3 ($P < 0.01$; Fig. 3C). Furthermore, the expression of OCN, a marker of late-stage differentiation, began to increase at day 7 by up to 2.75- and 3.45-fold ($P < 0.01$; Fig. 3D).

Next, we evaluated the ALP activity of osteoblast-like cells. As shown in Fig. 3E, OBAP significantly increased the ALP activity of osteoblast-like cells after 5 days of culture by up to 1.58- and 2.24-fold compared to vehicle-treated cells. These results indicate that OBAP stimulates osteoblast differentiation.

3.6. Effects of the novel peptide on BMD in vivo

To explore the *in vivo* effects of OBAP in the bone, we measured BMD by DXA in Gx rats. Seven-week-old male Gx rats were infused intraperitoneally with the novel peptide for 4 weeks. Compared with the vehicle control, OBAP significantly increased BMD in Gx rats (Fig. 4A–C).

3.7. Effects of the novel peptide on serum ALP and osteocalcin in Gx rats

To confirm the *in vivo* effects of OBAP on bone, we measured serum ALP and OCN in Gx rats. Compared with the vehicle control, OBAP significantly increased ALP and OCN in Gx rats by up to 1.51- and 3.25-fold ($P < 0.01$), respectively (Fig. 4D and E).

4. Discussion

In this study, we isolated a novel peptide from the rat stomach and termed this peptide osteoblast activating peptide (OBAP). Furthermore, we demonstrated that OBAP directly promotes osteoblast differentiation *in vitro* and increases BMD *in vivo*.

First, we searched for novel peptides that are produced in various organs, such as the brain, liver, kidney and small intestine, and act on osteoblasts, but were unable to isolate these putative peptides. Next we examined peptides in the stomach because the stomach produces physiologically active substances (e.g., ghrelin). Furthermore, the stomach is thought to play a role in bone metabolism, and it is well documented that surgically removing the whole stomach (gastrectomy) or the acid-producing part of the stomach (fundectomy) results in osteopenia [6–15]. In fact, gastrectomy-evoked bone loss was observed in young dogs in 1938 [7]. Although the phenomenon of gastrectomy-evoked osteopathy has been known for over 70 years, the mechanism remains poorly

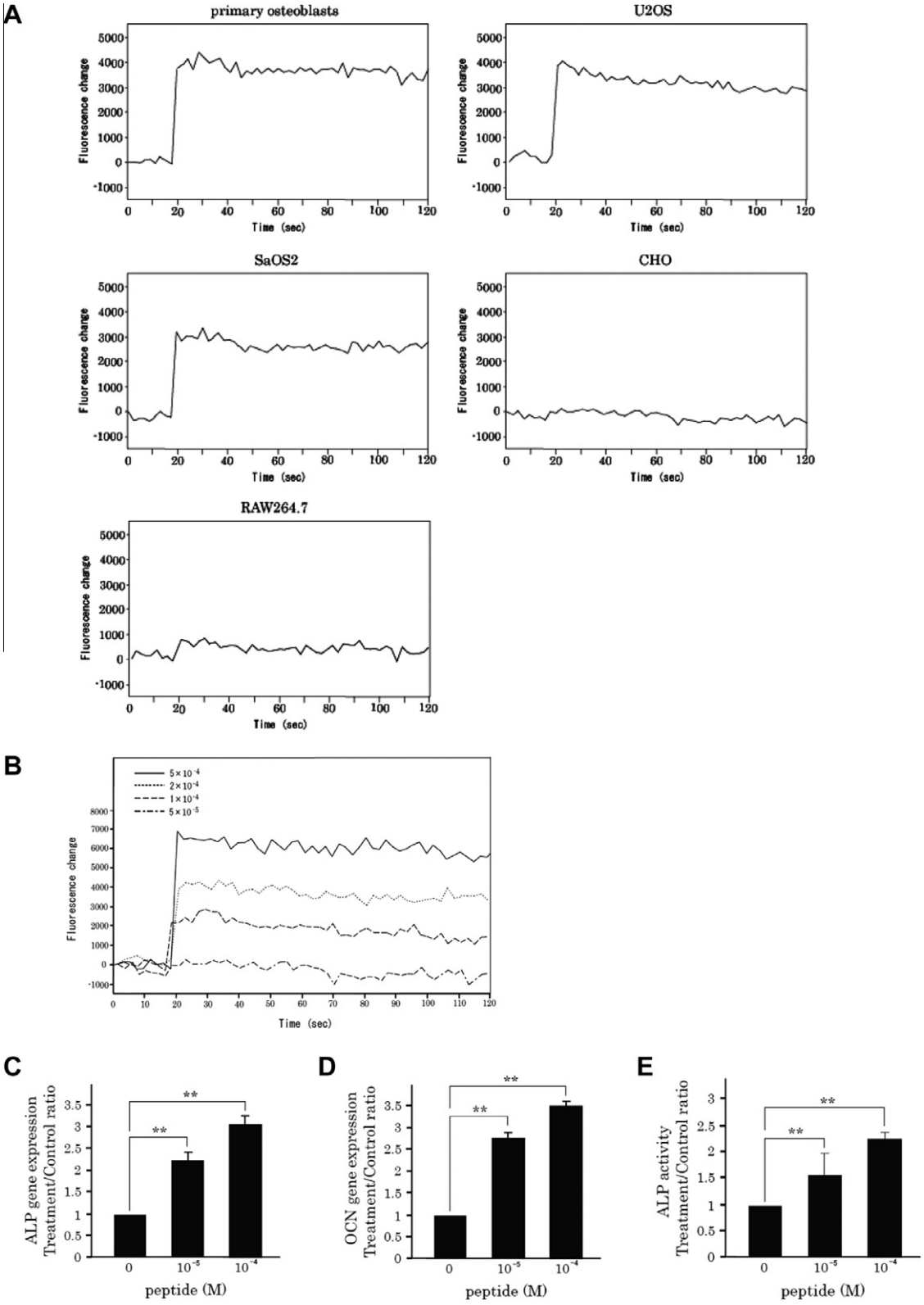

Fig. 3. Effects of the novel peptide *in vitro*. (A) Effects of the peptide on $[Ca^{2+}]i$ changes in osteoblastic cells (primary osteoblasts, U_2OS cells, and $SaOS_2$ cells), RAW264.7 cells, and CHO cells. (B) Dose-dependent response of $[Ca^{2+}]i$ changes in primary osteoblasts. $^{**}P < 0.01$ Quantitative RT-PCR analysis of the osteoblast differentiation marker genes (C) ALP and (D) OCN in cells treated with or without 10^{-5} and 10^{-4} M peptide. The novel peptide increased the expression of ALP and OCN. $^{**}P < 0.01$ (E) Dose-dependent effects of the novel peptide on ALP activity at day 5. Stimulating cells with 10^{-5} and 10^{-4} M peptide significantly increased ALP activity. $^{**}P < 0.01$.

understood. Previously, it was thought that bone loss was the result of an impaired capacity to utilize dietary calcium or a vitamin D deficiency. However, dietary supplementation with $CaCl_2$ [8,9] and continuous subcutaneous infusions of $CaCl_2$ [10] do not prevent bone loss, and 1,25-$(OH)_2D_3$ concentrations are reportedly increased rather than decreased after gastrectomies [11–14]. Based

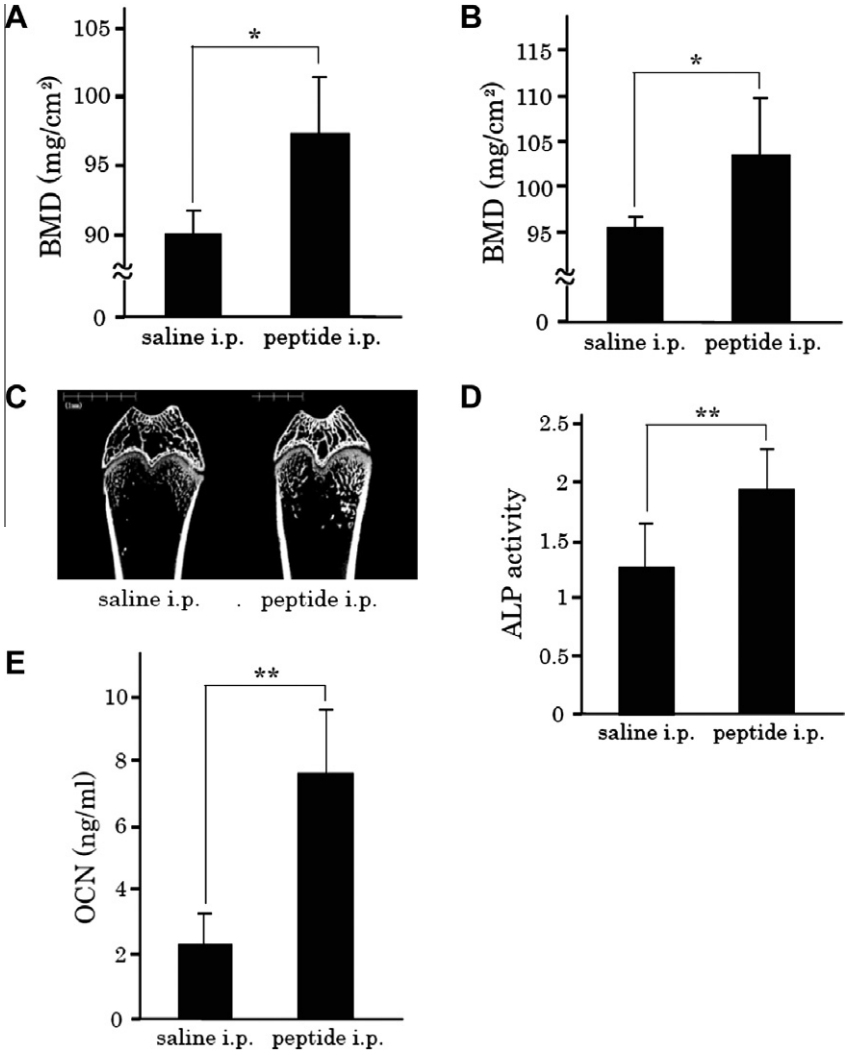

Fig. 4. Effects of novel peptide in gastrectomized rats. Rats were infused intraperitoneally with the peptide (0.2 mg/kg per hour, $n = 4$) or saline ($n = 5$) for 4 weeks. BMD was measured by DXA. The peptide treatment significantly increased both the (A) total and (B) trabecular BMD compared with saline treatment. $^{*}P < 0.05$ (C) Two-dimensional images of distal femurs by μCT. $^{*}P < 0.05$, $^{**}P < 0.01$ Effects of the novel peptide on serum alkaline phosphatase and osteocalcin in Gx rats. Rats were infused intraperitoneally with peptide (0.2 mg/kg per hour, $n = 4$) or saline ($n = 5$) for 4 weeks. Compared with the vehicle control, the peptide significantly increased (D) ALP and (E) OC. $^{**}P < 0.01$.

on these points, Larsson et al. suggested that ECL-cells harbor a novel peptide hormone that is involved in bone metabolism. In addition, they found that extracts of ECL-cell granule/vesicle enriched preparations of the oxyntic mucosa as well as extracts of isolated ECL cells evoked a typical Ca^{2+}-mediated second messenger response in different osteoblast-like cell lines [16,17]. We isolated OBAP, which is composed of 24 amino acids that are identical to the C-terminus of NADH dehydrogenase (ubiquinone) flavoprotein 3 (Ndufv3; MIPP65), which is a mitochondrial phosphoprotein [18] with an unknown function.

OBAP induced $[Ca^{2+}]i$ in primary osteoblasts and osteoblast-like cells but not RAW264.5 or CHO cells. These findings suggest that OBAP binds to a specific receptor in osteoblasts. To analyze the pharmacological activity of OBAP, we first measured osteoblast differentiation markers to confirm that OBAP potently affects osteoblasts. Furthermore, we demonstrated that OBAP increases ALP activity. These data confirm that OBAP stimulates osteoblast differentiation.

Next, we explored the *in vivo* effects of OBAP in the bone. It has been reported that PTH acts on osteoblasts, similar to the OBAP-induced increase in BMD [19]. These findings suggest that OBAP upregulates bone formation *in vivo*. In support of this hypothesis, we found that treating Gx rats with OBAP significantly increased BMD compared with saline treatment. We used Gx rats as an osteoporosis model because native peptide may be released by the stomach and enter the bloodstream, which could confound the effects of the native peptide.

OBAP resulted in a significant response *in vitro* and *in vivo*. However, if OBAP is used to treat osteoporosis, the effects should be stronger. Therefore, we need to further investigate and identify the OBAP receptor and improve the structure of OBAP to enhance its pharmacological effects.

The stomach is thought to play a role not only in bone metabolism but also in calcium metabolism. It is interesting that gastrin releases a hypocalcemic agent from the oxyntic mucosa and that subcutaneous injections of gastrin reduce blood calcium and stimulate Ca^{2+} uptake into the bone in rats [20–22]. Gastrin has been shown to induce hypocalcemia in thyroparathyroidectomized rats, indicating that calcitonin is not involved. However, gastrin does not affect bone calcium uptake in gastrectomized rats, whereas extracts of the oxyntic mucosa stimulate this process equally well in unmanipulated and gastrectomized rats [20]. These findings are thought to indicate that gastrin releases a hypocalcemic agent, currently referred to as gastrocalcin, from the oxyntic mucosa.

Because OBAP was purified and isolated from stomach and affects bone formation, it is possible that OBAP is gastrocalcin. Additional studies need to investigate this possibility.

In conclusion, we discovered a novel peptide, OBAP, which is a positive regulator that acts directly on osteoblasts. The discovery of OBAP may provide a new treatment option for osteoporosis and fracture healing.

Conflict of interest statement

All authors have no conflicts of interest.

Acknowledgments

We thank Hitomi Wakita, the hard tissue research team at Kureha Chemical Co. Ltd., and the technical team at Charles River Laboratories Japan for technical assistance. This work was supported by a Grant-in-Aid for Young Scientists (B) from the Japan society for the promotion of science (20791058), the Nakadomi foundation and the Ishibashi foundation for the promotion of science to N.F.

References

[1] L.S. Stepnick, The frequency of bone disease, in: J.A. McGowan, L.G. Raisz, A.S. Noonan, A.L. Elderkin (Eds.), Bone Health and Osteoporosis: A Report of the Surgeon General, Office of the US Surgeon General, Washington, DC, 2004, pp. 68–87.
[2] D. Shoback, Update in osteoporosis and metabolic bone disorders, J. Clin. Endocrinol. Metab. 92 (2007) 747–753.
[3] C.G. Bellows, J.E. Aubin, J.N. Heersche, Physiological concentrations of glucocorticoids stimulate formation of bone nodules from isolated rat calvaria cells in vitro, Endocrinology 121 (1987) 1985–1992.
[4] N. Fukushima, R. Hanada, H. Teranishi, Y. Fukue, T. Tachibana, H. Ishikawa, S. Takeda, Y. Takeuchi, S. Fukumoto, K. Kangawa, K. Nagata, M. Kojima, Ghrelin directly regulates bone formation, J. Bone Miner. Res. 20 (2005) 790–798.
[5] M. Kojima, H. Hosoda, Y. Date, M. Nakazato, H. Matsuo, K. Kangawa, Ghrelin is a growth-hormone-releasing acylated peptide from stomach, Nature 402 (1999) 656–660.
[6] Editorial, Osteomalacia after gastrectomy, Lancet 1 (1986) 77–78.
[7] R.A. Bussabarger, S. Freeman, A.C. Ivy, The experimental production of severe homogeneous osteoporosis by gastrectomy in puppies, Am. J. Physiol. 121 (1938) 137–148.
[8] F.I. Tovey, M.L. Hall, P.J. Ell, M. Hobsley, Postgastrectomy osteoporosis, Br. J. Surg. 78 (1991) 1335–1337.
[9] B. Klinge, D. Lehto-Axtelius, M. Åkerman, R. Håkanson, Structure of calvaria after gastrectomy. An experimental study in the rat, Scand. J. Gastroenterol. 30 (1995) 952–957.
[10] P. Persson, R. Gagnemo-Persson, D. Chen, J. Axelson, A.G. Nylander, O. Johnell, R. Håkanson, Gastrectomy causes bone loss in the rat: is lack of gastric acid responsible? Scand. J. Gastroenterol. 28 (1993) 301–306.
[11] L. Nilas, C. Christiansen, J. Christiansen, Regulation of vitamin D and calcium metabolism after gastrectomy, Gut 26 (1985) 252–257.
[12] J. Axelson, P. Persson, G. Gagnemo-Persson, R. Håkansson, Importance of the stomach in maintaining calcium homeostasis in the rat, Gut 32 (1991) 1298–1302.
[13] M. Davies, S.E. Heys, P.L. Selby, J.L. Berry, E.B. Mawer, Increased catabolism of 25-hydroxyvitamin D in patients with partial gastrectomy and elevated 1,25-dihydroxyvitamin D levels. Implications for metabolic bone disease, J. Clin. Endocrinol. Metab. 82 (1997) 209–212.
[14] G.W. Maier, M.E. Kreis, T.T. Zittel, H.D. Becker, Calcium regulation and bone mass loss after total gastrectomy in pig, Ann. Surg. 225 (1997) 181–192.
[15] D. Lehto-Axtelius, M. Stenström, O. Johnell, Osteopenia after gastrectomy, fundectomy, or antrectomy: an experimental study in the rat, Regul. Pept. 78 (1998) 41–50.
[16] B. Larsson, A. Gritli-Linde, P. Norlén, E. Lindström, R. Håkanson, A. Linde, Extracts of ECL-cell granules/vesicles and of isolated ECL cells from rat oxyntic mucosa evoke a Ca^{2+} second messenger response in osteoblastic cells, Regul. Pept. 97 (2–3) (2001) 153–161.
[17] B. Larsson, P. Norlén, E. Lindström, D. Zhao, R. Håkanson, A. Linde, Effects of ECL cell extracts and granule/vesicle-enriched fractions from rat oxyntic mucosa on cAMP and IP(3) in rat osteoblast-like cells, Regul. Pept. 106 (1–3) (2002) 13–18.
[18] M. Kitagawa, H. Mukai, Y. Ono, Molecular cloning and characterization of a novel mitochondrial phosphoprotein, MIPP65, from rat liver, Exp. Cell Res. 235 (1) (1997) 71–78.
[19] M.J. Mahon, M. Donowitz, C.C. Yun, G.V. Segre, Na(+)/H(+) exchanger regulatory factor 2 directs parathyroid hormone 1 receptor signalling, Nature 417 (6891) (2002) 858–861.
[20] P. Persson, R. Håkanson, J. Axelson, F. Sundler, Gastrin releases a blood calcium-lowering peptide from the acid-producing part of the rat stomach, Proc. Natl Acad. Sci. USA 86 (1989) 2834–2838.
[21] R. Håkanson, P. Persson, J. Axelson, O. Johnell, F. Sundler, Evidence that gastrin enhances ^{45}Ca uptake into bone through release of gastric hormone, Regul. Pept. 28 (1990) 107–118.
[22] R. Håkanson, P. Persson, J. Axelson, Elevated serum gastrin after food intake or acid blockade evokes hypocalcemia, Regul. Pept. 28 (1990) 131–136.